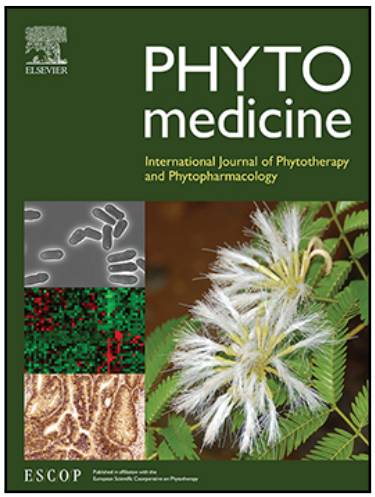

Candimine from Hippeastrum escoipense (Amaryllidaceae): Anti-Trypanosoma cruzi activity and synergistic effect with benznidazole

Javier E. Ortiz , Mauricio Piñeiro , Nieves Martines-Peinado , Patricia Barrera , Miguel Sosa , Jaume Bastida , Julio Alonso-Padilla , Gabriela E. Feresin

PII: S0944-7113(23)00149-6
DOI: https://doi.org/10.1016/j.phymed.2023.154788
Reference: PHYMED 154788

To appear in: *Phytomedicine*

Received date: 5 January 2023
Revised date: 10 March 2023
Accepted date: 27 March 2023

Please cite this article as: Javier E. Ortiz , Mauricio Piñeiro , Nieves Martines-Peinado , Patricia Barrera , Miguel Sosa , Jaume Bastida , Julio Alonso-Padilla , Gabriela E. Feresin , Candimine from Hippeastrum escoipense (Amaryllidaceae): Anti-Trypanosoma cruzi activity and synergistic effect with benznidazole, *Phytomedicine* (2023), doi: https://doi.org/10.1016/j.phymed.2023.154788

Highlights

- *Hippeastrum escoipense* is a potential source for the treatment of Chagas disease.
- Candimine decreases the cytotoxic effect of benznidazole in mammalian cells.
- Candimine induces alterations in the ultrastructure of *T. cruzi*
- The combination between candimine and benznidazole shows a synergistic effect in anti-*T. cruzi* assays.

Title: Candimine from *Hippeastrum escoipense* (Amaryllidaceae): Anti-*Trypanosoma cruzi* activity and synergistic effect with benznidazole

Authors: Javier E. Ortiz [a,b,1], Mauricio Piñeiro [a,b,1], Nieves Martines-Peinado [c,d], Patricia Barrera [e], Miguel Sosa [e], Jaume Bastida [d], Julio Alonso-Padilla [c,f,§], Gabriela E. Feresin [a,b,§*]

[a] Instituto de Biotecnología, Facultad de Ingeniería, Universidad Nacional de San Juan, Av. Libertador General San Martin 1109 O, San Juan, Argentina.

[b] Consejo Nacional de Investigaciones Científicas y Técnicas (CONICET), CCT CONICET San Juan

[c] Barcelona Institute for Global Health (ISGlobal), Hospital Clinic-University of Barcelona, 08036 Barcelona, Spain.

[d] Departament de Biologia, Sanitat i Medi Ambient, Facultat de Farmàcia i Ciències de l´Alimentació, Universitat de Barcelona, 08028 Barcelona, Spain.

[e] Facultad de Ciencias Médicas, Instituto de Histología y Embriología "Dr. Mario H. Burgos", Universidad Nacional de Cuyo-CONICET, CC 56 (5500) Mendoza, Argentina

[f] CIBER de Enfermedades Infecciosas, Instituto de Salud Carlos III (CIBERINFEC, ISCIII), Madrid, Spain.

[*]Corresponding author at: Instituto de Biotecnología, Facultad de Ingeniería, Universidad Nacional de San Juan, Av. Libertador General San Martin 1109 O, San Juan, Argentina.

E-mail address: gferesin@unsj.edu.ar (G.E. Feresin)

[1] Contributed equally to this study

[§] The work was co-directed by both authors

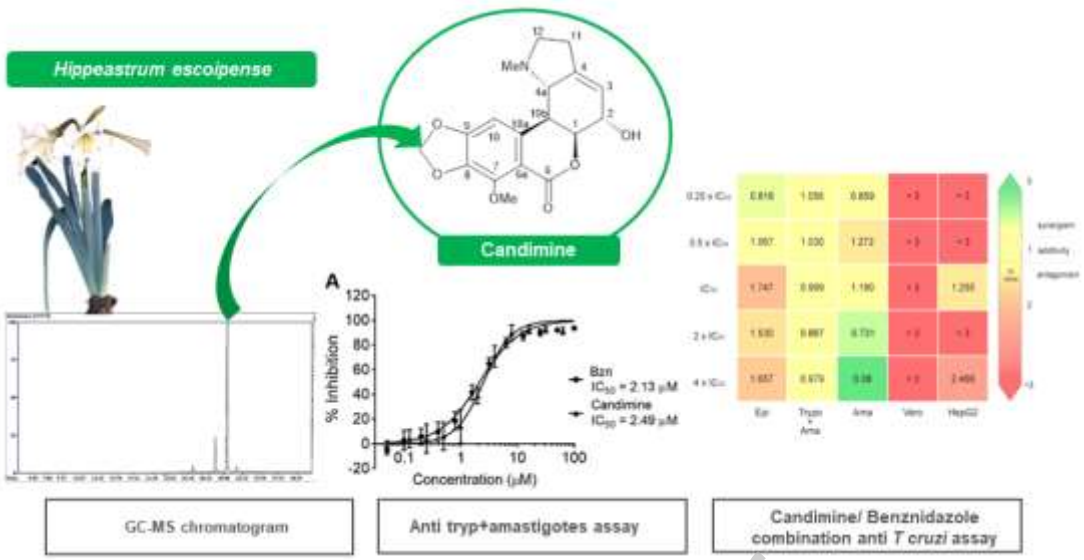

Abstract

Background: Chagas disease (CD), caused by *Trypanosoma cruzi*, represents a health threat to around 20 million people worldwide. Side effects of benznidazole (Bzn) cause 15-20% of patients to discontinue their treatment. Evidence has increased in favour of the use of drug combinations to improve the efficacy and tolerance of the treatment. Natural products are well known to provide structures that could serve as new drugs or scaffolds for CD treatment. Spp of the Amaryllidoideae sub family of Amaryllidaceae family are known by its bioactives alkaloids, which have a reported antiparasitic activity.

Purpose: To evaluate the anti-*T. cruzi* activity of the isolated alkaloid candimine (Cnd) from *Hippeastrum escoipense* Slanis & Huaylla; and to assess the combination effect between Cnd and Bzn against different life stages of *T. cruzi* parasites.

Methods: The chemical profile of *H. escoipense* alkaloids extract (AE-*H. escoipense*), including quantitation of Cnd was performed through GC/MS and UPLC-MS/MS techniques. Subsequently, Cnd was isolated using Shephadex LH20. Then, the AE-*H. escoipense* and Cnd were tested against *T. cruzi*, (epimastigotes, trypomastigotes, and amastigotes) by *in vitro* proliferation and viability assays. The cytotoxicity was evaluated against Vero and HepG2 mammalian cells. The ultrastructural analysis was perform by Transmission Electron Microcopy (TEM) and mitochondrial activity was carried out by MTT assay. Drug combination assay between Cnd and Bzn was evaluated using the Chou-Talalay method.

Results: The AE-*H. escoipense* and Cnd showed high and specific anti-*T. cruzi* activity, comparable to Bzn. Cnd induces ultrastructural changes in *T. cruzi*, such as vacuolization, membrane blebs and increases the mitochondrial activity. Regarding, the interaction between Cnd and Bzn generates synergism in the combinations of $0.25\times IC_{50}$ in epimastigotes, $2\times IC_{50}$ in trypomastigotes+amastigotes, and 0.25, 2, and $4\times IC_{50}$ in amastigotes.

Conclusion: The synergism between Cnd and Bzn indicates that the combination at the concentration of $4\times IC_{50}$ could be useful as an effective new therapy against CD in the chronic stage. Thus, Cnd isolated from the leaves of the *H. escoipense* emerges as potential candidate for the development of a new drug for the treatment of CD.

Keywords: Amaryllidaceae alkaloids, Chagas disease, antiparasitic assays, Neglected disease, Candimine, *Trypanosoma cruzi*.

Abbreviations:

AA: Amaryllidaceae Alkaloids
ACN: Acetonitrile
AE: Alkaloid Extract
ANOVA: Analysis of Variance
Bzn: Benznidazole
CD: Chagas Disease
CI: Combination Index
Cnd: Candimine
CPRG: Chlorophenol Red-β-D-Galactoside
DNA: Deoxyribonucleic Acid
DRI: Dose Reduction Index
DTU: Discreet Typing Units
ESI: Electrospray Ionization
Fa: Fraction affected
FBS: Fetal Bovine Serum
GC-MS: Gas Chromatography-Mass Spectrometry
IC_{50}: Half Maximal Inhibition Concentration
InC: Initial Concentration
LC-MS: Liquid Chromatography-Mass Spectrometry
MeOH: Methanol

MOI: Multiplicity of Infection

MTT: 3-[4,5-dimethylthiazol-2-yl]-2,5 diphenyl tetrazolium bromide

n°p: Number of Parasites

Nfx: Nifurtimox

NMR: Nuclear Magnetic Resonance

PBS: Phosphate Buffered Saline

RI: Retention Index

ROS: Reactive Oxygen Species

SI: Selectivity Index

SIR: single ion recording

TC_{50}: Half Maximal Toxicity Concentration

TEM: Transmission Electron Microscopy

TIC: Total Ion Current

UPLC-MS/MS: Ultra High-Performance Liquid Chromatography – Tandem Mass Spectrometry

WHO: World Health Organization

Introduction

About 6–7 million people worldwide, mostly in Latin America, are estimated to be infected with *Trypanosoma cruzi*, the parasite that causes Chagas disease (WHO, 2022). Currently available antiparasitic treatment is based on mono-pharmacology with nifurtimox (Nfx) or benznidazole (Bzn). They have shown very good efficacy against the acute stage of the infection, but this is mostly asymptomatic and usually goes undiagnosed and untreated. The diagnosis is generally made during the chronic stage, which is also when CD clinical signs at the heart and/or digestive tissues appear. By then, the efficacy of Bzn and Nfx is diminished and they have frequent side effects that cause treatment discontinuation in 15-20% of the patients. Therefore, new treatments with improved efficacy and safety are highly needed. In this regard, the research and use of combined therapy including natural compounds offer an opportunity to solve these pharmacological problems (Torrico *et al*., 2021).

Amaryllidoideae is a subfamily of Amaryllidaceae family, which synthesize isoquinoline-like alkaloids, known as Amaryllidaceae alkaloids, which have shown remarkable pharmacological properties including antiparasitic activity (Berkov *et al*., 2020; Martinez-Peinado *et al*., 2022; Nair and van Staden, 2023). The *Hippeastrum*

genus (Amaryllidaceae), in Argentina, comprises ten widely distributed and poorly studied species, among them *H. escoipense* (Zuloaga *et al*., 2008; Slanis *et al*., 2022;). The objective of this work was to evaluate the anti-*T. cruzi* activity of both the alkaloid extract of the *H. escoipense* Slanis & Huaylla and the main alkaloid candimine (Cnd). Furthermore, the combination effect between Cnd and Bzn was studied.

Material and methods

General experimental procedures

The GC-MS analysis were performed on an Agilent 6890N GC 5975 instrument (Agilent Technologies, Santa Clara, CA, USA) operating in EI mode at 70 eV. A DB-5 MS column (30 m x 0.25 mm x 0.25 μm) was used. The temperature program was: 100-180 °C at 15 °C min^{-1}, 1 min hold at 180 °C, 180-300 °C at 5 °C min^{-1}, and 1 min hold at 300 °C. The injector temperature was 280 °C. The flow rate of carrier gas (He) was 0.8 ml min^{-1}. The split ratio was 1:20. The results obtained were analysed using AMDIS 2.64 software. Compounds were identified by comparing their mass spectral patterns and retention index (RI) with those of more than 300 previously isolated alkaloids spectra in homemade databases (a private Amaryllidaceae alkaloid library) (Berkov et al., 2020). RIs were calculated through calibration with a standard *n*-hydrocarbon mixture (C_9−C_{36}). Results are expressed as a percentage of total ion current (TIC) in each chromatogram, which was used for comparison of relative abundance among the components of the extract. The LC-MS analysis were performed on an ACQUITY *H*-Class UPLC equipped with a XEVO TQ-S micro triple quadrupole mass spectrometer (Waters Corp, Milford, MA, USA) with electrospray ionization (ESI). An UPLC ACQUITY BEH C18 (1.7 μm, 2.1 mm×50 mm) column was used for separation at 38 ºC. The mobile phase consisted of water (0.1 % formic acid), ACN (0.1 % formic acid), and MeOH with a flow rate of 0.2 ml/min. The gradient conditions were as follows: 0–2 min, 95 % water-5 % ACN; 2–5 min, 85 % water–15 % ACN; 5–10 min, 80 % water – 10 % ACN – 10 % MeOH and hold for 7 min, 17–18 min, 95% water – 5% ACN and hold for 2 min; completing 20 min. The calibration curve was constructed by using five standard solutions of Cnd (0.1, 1, 5, 7.5, and 10 ppm) in triplicate. The AE-*H. escoipense* was prepared at 100 ppm. The samples were dissolved in a mixture of methanol:water (50:50) and filtered through a

membrane filter (0.22 µm). The injection volume was 10 µL. The data were acquired using the single ion recording (SIR) mode, and processed using MassLynx Software V4.2 (TargetLynx^{TM}, Waters, Milford, MA, USA). The NMR ^{1}H and ^{13}C spectra were recorded on a Mercury 400 MHz (Palo Alto, CA, USA) and a Varian 500 MHz (Palo Alto, CA, USA) instruments using $CDCl_3$ as solvent.

Plant material

The leaves of *Hippeastrum escoipense* Slanis & Huaylla were collected in northwest of Argentina (25°10'08.0"S, 65°44'09.6"W), between the years 2020-2022 during the flowering period. To contribute to the conservation and sustainable use of biological resources just some samples involving the whole plant were collected for identification purposes. These samples were authenticated by Lic. A. Slanis and vouchers of the specimen were deposited at the Herbario Miguel Lillo (holotipo, LIL-617830 [004008], isotipos LIL- 617830 [004009, 004010, 004011, 004012]) according to Slanis *et al*. (2022).

Alkaloids extraction and isolation of Cnd

Dried leaves (60 g) were powdered and extracted three times with MeOH under reflux for 1 h. The solvent was evaporated under reduced pressure to obtain the crude MeOH extract. The extract was dissolved in 2% H_2SO_4 (v/v), and neutral material was removed three times with Et_2O. Then, the aqueous solution was basified with 25% NaOH to pH 10-11 and extracted three times with $CHCl_3$ to give the *H. escoipense* alkaloid extract (AE-*H. escoipense*) (65 mg). Column chromatography on Sephadex LH–20 of the alkaloid extract in MeOH gave three fractions (A-C). Direct crystallization from the fraction B yielded 2.5 mg of Cnd.

***Trypanosoma cruzi* culture**

T. cruzi epimastigotes (Dm28c strain – DTU: TcI) were cultured at 28 °C in Diamond medium (0.1 M NaCl, 0.05 M K_2HPO_4, 0.625 % tryptose, 0.625 % tryptone, 0.625 % yeast extract, pH 7.2), supplemented with 10 % inactivated FBS (Gibco) and 12.5 µg/ml hemin and antibiotics 0.1 % (penicillin 75 U/ml and streptomycin 75 µg/ml). *T. cruzi* trypomastigotes and amastigotes (Tulahuen-β-gal strain – DTU: TcVI) were kept in culture using LLC-MK2 cells as host as previously described (Martinez-Peinado *et al*., 2020).

Host cells cultures

Vero (green monkey kidney epithelial cells) and HepG2 (human liver epithelial cells) were maintained as described (Martinez-Peinado *et al*., 2020).

Proliferation and viability of *T. cruzi* assay

Epimastigotes were incubated at 28°C in sterile plastic tubes with different concentrations of AE-*H. escoipense* (1 to 10 µg/ml) and Cnd (1.41 to 14.1 µM). The initial concentration (InC) of parasites was 3×10^6/ml in a final volume adjusted to 1 ml. The negative controls were parasites without treatment; and the positive control was Bzn (5 µg/ml/19.2 µM). Following the protocol of Spina *et al*. (2018), aliquots were collected at 24, 48, and 72 h, and they were suspended in 2 % p-formaldehyde in PBS (0.15 M NaCl, 0.02 M NaH_2PO_4, 0.017 M NaOH; pH 7.2). Then the number of parasites (n° p) was counted in a Neubauer chamber. The percentage of inhibition was calculated as:

$$\% \text{ inhibition} = 100 - \{[(n° \text{ p treated} - \text{InC})/(n° \text{ p control} - \text{InC})]*100\}$$

The anti-trypomastigotes+amastigotes assay against *T. cruzi* infective stages was performed as reported previously (Martinez-Peinado *et al*., 2020). Test plates were prepared with starting concentrations of 1050 µg/ml of extract or 125 µM of compound, which were diluted 1:2 following a concentration-response pattern. Vero cells and purified trypomastigotes at a concentration of 1×10^6/ml were mixed at a 1:1 volume: volume ratio and 100 µl of the solution were added *per* well (50,000 Vero cells and 50,000 trypomastigotes; multiplicity of infection or MOI = 1). Bzn was included as positive control. Plates were incubated for 4 days at 37 ºC and assay readout was performed with chlorophenol red-β-D-galactoside (CPRG) substrate.

Anti-amastigote of *T. cruzi* specific assay

An anti-amastigote assay was performed as previously reported Martinez-Peinado *et al*. (2020). Succinctly, 5×10^6 Vero cells were seeded in a T-175 flask and cultured for 24 h. Then, cells were infected with 1×10^7 trypomastigotes (MOI ~ 1) and the inoculum left for 18 h. After that, infected cell monolayers were washed with PBS and detached from the flask. Cells were diluted to a concentration of 5×10^5 cells/ml and 100 µl of the solution were added per well to test plates already containing the extract or Cnd. Bzn was included as control drug.

Toxicity assays with Vero and HepG2 cells

Vero and HepG2 cells toxicity assays were performed as described Martinez-Peinado *et al*. (2020). Briefly, Vero and HepG2 cells were respectively diluted at concentrations of 5×10^5 and 3.2×10^5 cells/ml. Then, 100 µl of the cell solution were added *per* well to test plates already containing either the extract or alkaloid. Each run contained its own negative and positive controls. Plates were incubated at 37 ºC for 4 days in the case of Vero cells, and 2 days for HepG2 cells. Then, 50 µl *per* well of a PBS solution containing 10 % alamarBlue reagent was added and plates were incubated for 6 h at 37 ºC before reading the fluorescence intensity (excitation: 530 nm, emission: 590 nm). For further progression of the anti-*T. cruzi* experiments sequence, only the results with selectivity index (SI, or TC_{50} to IC_{50} ratio) > 10 were considered (Martinez-Peinado *et al*., 2020).

Ultrastructural analysis by transmission electron microscopy (TEM)

The ultrastructural study was carried out according to Spina *et al*. (2018). Briefly, treated (Cnd 7.07 and 14.1 µM) or non-treated *T. cruzi* epimastigotes were collected, centrifuged at 3,000 rpm, and fixed with 2 % glutaraldehyde in PBS (24 h at 4 °C). Parasites were washed twice with PBS, and then incubated overnight with 1 % osmium tetroxide at 4 °C. Again, epimastigotes were washed twice, dehydrated with increasing concentrations of acetone, and pre-infiltrated in a 1:1 solution of acetone and Spurr Low Viscosity Kit Ted Pella resin for 2 h. Parasites were then centrifuged and embedded in pure Spurr Low Viscosity Kit Ted Pella resin for 24 h at 60 °C. Ultrathin sections were cut with a Power Tone XL ultramicrotome and contrast-stained with uranyl acetate and lead citrate. Samples were analysed in an EM 900 Zeiss electron microscope.

Mitochondrial activity

Epimastigotes (3×10^6/ml) were treated with 28.29 µM Cnd for 48 h. Parasites were then centrifuged at 3,000 rpm for 10 min. The parasites-containing pellet was resuspended in 100 µl of Diamond medium and 10 µl MTT (5 mg/ml) with phenazine methosulfate (0.22 mg/ml) in PBS and incubated for 4 h at 28 °C. The suspension was then centrifuged, and the medium removed. The precipitate was dissolved with 100 µl of DMSO and the absorbance was measured at 570 nm using a FC® Microplate Photometer, Thermo Scientific (Spina *et al*., 2018).

Drug combination assay

The IC_{50} value was first determined for Cnd and Bzn, each one alone in different cells types. Then Cnd and Bzn were combined in a fixed ratio (1:1) for different concentrations based on both IC_{50} values as follows: ($0.25\times IC_{50}$ Cnd + $0.25\times IC_{50}$ Bzn), ($0.5\times IC_{50}$ Cnd + $0.5\times IC_{50}$ Bzn), ($1\times IC_{50}$ Cnd +$1\times IC_{50}$ Bzn), ($2xIC_{50}$ Cnd + $2\times IC_{50}$ Bzn), ($4\times IC_{50}$ Cnd + $4\times IC_{50}$ Bzn). (Fig. S1). To quantify drug interaction between Cnd and Bzn, the Combination Index (CI), Fraction affected (Fa) and Dose Reduction index (DRI) were estimated by the unified theory, introduced by Chou and Talalay (Chou, 2010) using CompuSyn software. The CI is a quantitative representation of pharmacological interactions. CI < 1 indicates synergism, CI = 1 additive interaction, and CI > 1 antagonism. The Fa is a value between 0 and 1, where 0 means that the drug had no effect on cell viability and 1 means that the drug had a total effect on decreasing cell viability. The DRI is a dimensionless measure of how fold the dose of each drug in a combination may be reduced compared with the dose of each drug alone. Where, DRI > 1 indicates favourable dose reduction, DRI < 1 unfavourable dose reduction and finally DRI = 1 indicates no dose reduction (Chou, 2010, Chen *et al.*, 2023).

Data analysis

The Student's t was used to determine the statistical significance of the difference between treated and control groups. The effect of each treatment was analysed by one-way analysis of variance (ANOVA). IC_{50} and TC_{50} values to single compound/extract were determined with GraphPad Prism 7 software (version 7.00, 2016) using a non-linear regression analysis model ([Inhibitor] vs. normalized response - Variable slope) (Martinez-Peinado *et al.*, 2020). All the experiments were performed at least in triplicate. To quantify drug interaction, the CompuSyn software (ComboSyn, Inc., New York, New York state, USA) was used. The mutually exclusive model was used, based on the assumption that drugs act through entirely different mechanisms.

Results

Chemical analysis

The alkaloids lycorine, Cnd, and 2-hydroxyhomolycorine were identified in AE-*H. escoipense* by means of GC-MS. The ions with a m/z 341 and 355 were not identified through the library match process (Fig. S2). Although GC-EI-MS represents a useful

and reliable tool for AA identification throughout the use of libraries, it is possible that some alkaloids could not be detected. (e.g., non-volatile compounds). In order to better understand the AE-*H. escoipense* composition, an UPLC-ESI-MS analysis was performed. This technique has the advantage to detect certain compounds, such as non-volatile, high temperature susceptible alkaloids and other conditions applied in GC-MS method (Fig.S2, S3). The UPLC-MS/MS analysis showed the $[M+H]^+$ ions corresponding to the alkaloids previously identified by GC-MS including the alkaloid Cnd at m/z 346. However, significant variations in each compound abundance were observed in the chromatogram and the presence of other alkaloids with $[M+H]^+$ values of 380, 364, 362, and 266 not identified in GC-MS analysis, were also detected (Fig. S3).

The structure of Cnd was confirmed by ^1H and ^{13}C NMR spectroscopy, and the results were in agreement with literature data. The melting point was determined for Cnd showing a value of 210°C (Electrothermal™ IA9000 Series, Thermo Fisher Scientific, UK). Based on the ^1H NMR data, the purity of candimine was >95%. (Fig. S4, S5). In order to understand the content of Cnd, an UHPLC-MS/MS quantitative analysis was performed for the AE-*H. escoipense* given a value of 7.9 ± 0.8 % (w/w). The linear correlation curve was r2 = 0.9918, and the linear equation was y = 137.130 x + 0.85.

Anti-*T cruzi* activity

The IC_{50} values of AE-*H. escoipense* against *T. cruzi* were 2.63 and 1.62 ± 0.03 µg/ml for the epimastigotes and trypomastigotes+amastigotes stages, respectively (Table 1, Fig. 1 and 2A). Then, the Vero cell toxicity assay to test for its parasite specific activity showed a TC_{50} = 30.28 ± 3.28 µg/ml with a SI of 18.72 (Table 1, Fig. 2B). The HepG2 cell toxicity assay reported a TC_{50} value of 10.9 ± 1.20 µg/ml (Table 1, Fig. 2C). Finally, the AE-*H. escoipense* showed a specific anti-amastigote activity of TC_{50} = 1.42 ± 0.09 µg/ml, reaching a SI of 21.32 (Table 1, Fig. 2D). The IC_{90}.values were included in Table 1.

Considering the GC-MS alkaloid profile, the study was aimed to find out the contribution of each identified alkaloid to the anti-*T. cruzi* activity of the AE-*H escoipense*. Thus, the isolation process from the AE-*H escoipense* was performed. The anti-*T. cruzi* activity of Lycorine was reported by Martinez-Peinado et al. (2020). The alkaloid 2-hydroxyhomolycorine was detected in a very low proportion and, considering the yield of the AE-*H escoipense*, it could not be isolated. As a result, only

the alkaloid Cnd (Fig. 3) was obtained with a high level of purity, and it was then evaluated for its anti-*T. cruzi* activities in the same manner than previously described for the AE-*H escoipense*. The inhibitory effect of Cnd on the proliferation of *T. cruzi* epimastigotes was concentration-dependent showing an IC_{50} value lower than that of Bzn (4.28 ± 0.47 µM and 8.21 ± 1.4 µM at 48 h, respectively) (Table 1) (Fig. 4). Likewise, Cnd showed an IC_{50} value of 2.49 ± 0.16 µM against trypomastigotes+amastigotes, being similar to that of Bzn (Table 1, Fig. 5A). The anti-amastigote activity of Cnd , was IC_{50} = 1.60 ± 0.15 µM (Table 1, Fig. 5D). In addition, the Vero cell toxicity assay showed a TC_{50} = 255.4 ± 74.93 µM for Cnd, indicating less toxicity than Bzn (Table 1, Fig. 5B). Its low toxicity in the Vero cells assay led to obtain SI values of 69.67, 102.57, and 159.63 for epimastigotes, trypomastigotes+amastigotes, and amastigotes stages, respectively (Table 1). Finally, in HepG2 cells assay, Cnd showed a TC_{50} = 85.17 ± 15.49 µM (Table 1, Fig. 5C).

Regarding the parasite ultrastructure analysis by TEM, Cnd induced several ultrastructural alterations on epimastigotes (Fig. 6). The treatment with 7.07 µM showed high vacuolization (Fig. 6B). Likewise at 14.1 µM) reservosome-like structures throughout the cytoplasm and plasmatic membrane blebs, were observed (Fig. 6C). In regard to the MTT analysis, Cnd induced a significant increase in the mitochondrial activity of *T. cruzi* epimastigotes with respect to the control of untreated parasites (0.059 ± 0.006 and 0.047 ± 0.005, respectively) (Fig. 7).

Synergistic effect

The combination of Cnd and Bzn showed a concentration-dependent activity on epimastigotes, trypomastigotes+amastigotes, and amastigotes (Fig. 8A-C). In the epimastigote forms, the interaction of the drugs resulted in a synergistic effect (CI < 1) only for the combination of 1.07 µM of Cnd and 2.05 µM of Bzn (Table 2, Fig. 8D). All the combinations resulted in a favourable reduction in Bzn concentrations (Table 2, Fig. 8H). In trypomastigotes+amastigotes culture, four of five combinations showed an interaction between Cnd and Bzn at the threshold of additive affect (0.9 < CI < 1.1), although for the combination of 2 × IC_{50} (4.28 µM and 3.74 µM, respectively) a slight synergistic effect was observed (CI = 0.867) (Table 2, Fig. 8E). In epimastigotes, all combinations showed a favourable reduction in the concentration of Bzn as well as Cnd (DRI > 1) (Table 2, Fig. 8H). In the case of the amastigotes-specific assay, three combinations showed a synergistic interaction between Cnd and Bzn (CI < 1),

highlighting the drug combo in the relationship of $4\times IC_{50}$ with an CI value equal to 0.08 (Table 2, Fig. 8F) and with a reduction concentration of Bzn of 17.6 times. On the other hand, all combinations showed a favourable reduction in the concentration of Bzn as well as Cnd, with a more marked effect at higher concentrations (DRI > 1) (Table 2, Fig. 8I). Finally, the compounds interaction in Vero and HepG2 cells at all the combinatorial ranges, presented an antagonistic effect (CI >1) (Table 2, Fig. 9). The CI values obtained from all the combinations in the different cell types are represented in the heat map of figure 9. The results obtained by the algorithm of the Chou-Talalay method match with those of the classic isobologram method (Fig. S8).

Discussion

In this study, it was found that AE-*H. escoipense* specifically inhibited the growth of *T. cruzi* in all the antiparasitic assays performed. It showed low toxicity against Vero cells and HepG2 cells and was more active than Bzn against the amastigote forms (Table 1). Although SI of the AE-*H. escoipense* were lower than those of Bzn for all stages of *T. cruzi*, the retrieved results are above the values stipulated by Martinez-Peinado *et al*. (2020) (SI > 10) to consider it was specifically acting on the trypanosome forms. Cnd had high activity against *T. cruzi* forms (Table 1). In epimastigotes, Cnd was almost twice more effective than Bzn. Additionally, the effect of Cnd on the ultrastructure and mitochondrial activity of epimastigotes was evaluated in an attempt to elucidate its possible mechanism of action. Electron microscopy has proven to be a reliable and essential tool to determine morphological alterations and target organelles in the investigation of new drugs for Chagas disease (Menna-Barreto *et al*., 2009).

After 48 h of treatment with 7.07 and 14.1 µM of Cnd, the parasites showed several changes in its ultrastructure, as such intense vacuolization, membrane blebs and reservosome-like structures (RLS) disorganization (Elso *et al*., 2022). The appearance of RLS could be related to alterations of parasite metabolism (reviewed by Menna-Barreto et al., 2012). Some of these alterations, mainly internal and cytoplasmic membrane vacuolization, were observed in *Trichomonas vaginalis* treated with Cnd at 250 µM for 6 and 24 h, suggesting paraptotic cell death (Giordani *et al*., 2010). Despite that *T. cruzi* must deal with high reactive oxygen species (ROS) levels generated as part of the host's immune responses and with those ROS produced by its

own metabolism, the parasites have limited ability to fight against ROS. Since mitochondrion is one of the major sources of reactive oxygen species (ROS) this organelle has been described as a potential target of novel drugs due to the absence of classical antioxidant defences (Spina et al., 2018; Bombaça et al., 2019).

Although *T. cruzi* treated with Cnd did not present ultrastructural alterations in the mitochondrion, an increase in mitochondrial activity was observed by means of the MTT assay in the parasites incubated with 14.1 μM of Cnd. This could be consistent with an increase in the metabolism of the parasite to provide protection against cell damage as suggested by Wilkinson *et al*. (2000). Regarding the kinetics of the growth curve, Giordani *et al*. (2010) reported that Cnd arrests the cell cycle of *T. vaginalis* in the G2 phase. This could explain the inhibition of cell division observed in the *T. cruzi* treated with Cnd.

The alkaloid Cnd had selective activity against the *T. cruzi* infective forms and very low toxicity against Vero and HepG2 mammalian cells. The *T. cruzi* amastigotes were the most sensitiveto Cnd, and showed a better SI than Bzn (159.63 and 147.55, respectively). Regarding the anti-*T. cruzi* activity of Cnd vs AE-*H. escoipense*, it was found that the alkaloid Cnd was 1.78, 1.98, and 2.78-fold more active for epimastigotes, trypomastigotes+amastigotes, and amastigotes, respectively. On the other hand, hippeastrine, another alkaloid belonging to the Amaryllidaceae family, showed a lower anti-*T. cruzi* activity (Martinez-Peinado *et al*., 2020), and although it presents a very similar structure to that of Cnd, it differs in the absence of a CH_3O group at the C-7 position. Thus, it is very likely that the antiparasitic activity of Cnd can be due to this difference (Fig. 3). The effect of the methoxy group occurring in several compounds showing activity against *T. cruzi* and other trypanosomatids such as *T. brucei* and *L. mexicana*, has been reported (Izumi *et al*., 2011; Alotaibi *et al*., 2021). Souza *et al*. (2021) showed that the anti-*T. cruzi* activity can be improved by replacing the highly reactive β-diketone functionality in the curcumin structure by selective addition of methoxy groups on the terminal aromatic rings. This structural configuration could facilitate the formation of the extended phenoxy radical ROS with the participation of the oxygen of the methoxy group (Litwinienko and Ingold, 2004).

Combination therapy for CD could be a promising alternative that might improve the efficacy of drugs by targeting multiple metabolic pathways and reducing the side effects as well as the risk of the appearance of drug resistance events (Hernández *et*

al., 2021). In this study, the *in vitro* assay combining Cnd and Bzn showed at least one synergistic interaction for each of the parasite stages. In epimastigotes, such synergistic interaction was given by the combination of low concentrations of Cnd and Bzn. Regarding the antiparasitic performance in the trypomastigotes+amastigotes assay, general interactions of the drugs resulted in additivity, with a slight synergism at $2\times IC_{50}$ concentrations. Remarkably, the combination of $2\times IC_{50}$ and $4\times IC_{50}$ stood out in the anti-amastigotes assay for its potent synergism (CI = 0.731 and 0.08, respectively). Indeed, when *T. cruzi* was treated with combinations of Cnd and Bzn, a potent synergistic interaction was observed for some of the combinations. However, all of these combinations showed a concentration reduction of Bzn (DRI > 1) when evaluated against all *T. cruzi* stages. In addition, the combination of Cnd and Bzn were antagonistic for Vero and HepG2 cells, indicating a decrease in the cytotoxicity of both drugs when they act together.

Barrett *et al*. (2019) described the ability of amastigotes to remain in latency in tissues. During the chronic phase of the CD, the dormant parasites metabolism is reduced and may be less susceptible to drug action (Villalta *et al*., 2019). In this study, Cnd showed both alone and combined with Bzn, a potent effect especially against amastigotes forms. Therefore, it would be of interest to perform further experiments specifically targeting these parasite forms with Cnd.

Conclusions

The AE-*H. escoipense* and Cnd are potent anti-*T.cruzi* agents. Considering the toxicity against Vero cells, Cnd presents a better SI than Bzn for all the parasitic stages evaluated. In addition, Cnd and Bzn showed a synergistic effect against *T. cruzi*, reducing the concentration of Bzn up to 17.6 times and presenting a powerful synergistic interaction in amastigotes forms. Further research is needed to find potential targets of Cnd as well as its mechanism of action against the parasite. Finally, *H. escoipense* represents a renewable source of candimine justifying future *in vivo* trials. In order to protect biodiversity, propagation studies will be carried out to obtain candimine from greenhouse crops.

Acknowledgments

M.P. and J.O. hold a fellowship from CONICET. G.E.F. is researcher from CONICET. N.M.P. work was supported by the ISCIII project PI18/01054. And to

Slanis A. C. and Huaylla H. by the identification of the species and provided the samples.

References

Aguilera, E., Varela, J., Serna, E., Torres, S., Yaluff, G., Bilbao, N.V.D., and González, M. (2018). Looking for combination of benznidazole and *Trypanosoma cruzi*-triosephosphate isomerase inhibitors for Chagas disease treatment. Mem. Inst. Oswaldo Cruz 113, 153–160. DOI: 10.1590/0074-02760170267.

Alfayez, I.A., Natto, M.J., Alenezi, S., Siheri, W., AlQarni, M., Igoli, J.O., Fearnley, J., De Koning, H.P., and Watson, D.G. (2021). Activity of compounds from temperate propolis against *Trypanosoma brucei* and *Leishmania mexicana*. Molecules 26, 3912. DOI: 10.3390/molecules26133912.

Álvarez, M.G., Hernández, Y., Bertocchi, G., Fernández, M., Lococo, B., Ramírez J.C., Cura. C., Albizu, C.L., Schijman, A., Abril, M., Sosa-Estani, S., and Viotti, R. (2020). New scheme of intermittent benznidazole administration in patients chronically infected with *Trypanosoma cruzi*: clinical, parasitological, and serological assessment after three years of follow-up. Antimicrob. Agents Chemother. 64, e00439–20. DOI: 10.1128/aac.00745-15.

Barrett, M.P., Kyle, D.E., Sibley, L.D., Radke, J.B., and Tarleton, R.L. (2019). Protozoan persister-like cells and drug treatment failure. Nat. Rev. Microbiol. 17, 607–620. DOI: 10.1038/s41579-019-0238-x.

Bastida, J., Lavilla, R., and Viladomat, F. (2006). Chemical and biological aspects of *Narcissus* alkaloids. In: Cordell GA (ed), The Alkaloids: The Alkaloids. Chemistry and biology. Elsevier, Amsterdam 63, 87–179. DOI: 10.1016/s1099-4831(06)63003-4 DOI: 10.1016/s1099-4831(06)63003-4.

Berkov, S., Osorio, E., Viladomat, F., and Bastida, J. (2020). Chemodiversity, chemotaxonomy and chemoecology of Amaryllidaceae alkaloids 83, 113–185. In: Alkaloids Chem. Biol. DOI: 10.1016/bs.alkal.2019.10.002.

Bern, C. (2011). Antitrypanosomal therapy for chronic Chagas' disease. N. Engl. J. Med. 364, 2527–2534. DOI: 10.1056/NEJMct1014204.

Bombaça, A.C.S., Viana, P.G., Santos, A.C., Silva, T.L., Rodrigues, A.B.M., Guimarães, A.C.R., Goulart M.O.F., da Silva Júnior, E.N., and Menna-Barreto, R.F. (2019). Mitochondrial disfunction and ROS production are essential for anti-*Trypanosoma cruzi* activity of β-lapachone-derived naphthoimidazoles. Free Radic. Biol. Med. 130, 408–418. DOI: 10.1016/j.freeradbiomed.2018.11.012.

Chen, S., Xin, Y., Tang, K., Wu, Y., and Guo, Y. (2023). Nardosinone and aurantio-obtusin, two medicine food homology natural compounds, are anti-influenza agents as indicated by transcriptome signature reversion. Phytomedicine, 108, 154515. DOI:10.1016/j.phymed.2022.154515

Chou, T.C. (2010). Drug combination studies and their synergy quantification using the Chou-Talalay method. Cancer Res. 70, 440–446. DOI: 10.1158/0008-5472.CAN-09-1947.

Elso, O.G., Puente, V., Barrera, P., Sosa-Escudero, M.A., Sülsen, V.P., and

Lombardo, M.E. (2022). Mode of action of the sesquiterpene lactones eupatoriopicrin and estafietin on *Trypanosoma cruzi*. Phytomedicine 96, 153900. DOI: 10.1016/j.phymed.2021.153900.

Giordani, R.B., Vieira, P.B., Weizenmann, M., Rosember, D.B., Souza, A.P., Bonorino, C., de Carli, G.A., Bogo, M.R., Zuanazzi, J.A.S., and Tasca, T. (2010). Candimine-induced cell death of the amitochondriate parasite *Trychomonas vaginalis*. J. Nat. Prod. 73, 2019–2023. DOI: 10.1021/np100449g.

Giordani, R.B., de Andrade, J.P., Verli, H., Dutilh, J.H., Henriques, A.T., Berkov, S., Bastida, J., and Zuanazzi, J.A. (2011). Alkaloids from *Hippeastrum morelianum* Lem. (Amaryllidaceae). Magn. Reson. Chem. 49, 668–672. DOI: 10.1002/mrc.2794.

Hardy, K. (2021). Paleomedicine and the evolutionary context of medicinal plant use. Rev. Bras. Farmacogn. 31, 1–15. DOI: 10.1007/s43450-020-00107-4.

Hernández, M., Wicz, S., Caballero, E.P., Santamaría, M.H., and Corral, R.S. (2021). Dual chemotherapy with benznidazole at suboptimal concentration plus curcumin nanoparticles mitigates *Trypanosoma cruzi*-elicited chronic cardiomyopathy. Parasitol. Int. 81, 102248. DOI: 10.1016/j.parint.2020.102248.

Izumi, E., Ueda-Nakamura, T., Dias Filho, B.P., Júnior, V.F.V., and Nakamura, C.V. (2011). Natural products and Chagas' disease: a review of plant compounds studied for activity against *Trypanosoma cruzi*. Nat. Prod. Rep. 28, 809–823. DOI: 10.1039/c0np00069h.

Komolafe, K., Komolafe, T.R., Fatoki, T.H., Akinmoladun, A.C., Brai, B., Olaleye, M.T., and Akindahunsi, A.A. (2021). Coronavirus disease 2019 and herbal therapy: pertinent issues relating to toxicity and standardization of phytopharmaceuticals. Rev. Bras. Farmacogn. 31, 142–161. DOI: 10.1007/s43450-021-00132-x.

Laboratorios Liconsa. Package insert: benznidazole tablets, for oral use. (2017). https://www.accessdata.fda.gov/drugsatfda_docs/label/2017/209570lbl.pdf. Accessed 15th Sep. 2022.

Litwinienko, G., and Ingold, K.U. (2004). Abnormal solvent effects on hydrogen atom abstraction. 2. Resolution of the curcumin antioxidant controversy. The role of sequential proton loss electron transfer. J. Org. Chem. 69, 5888–5896. DOI: 10.1021/jo049254j.

Martínez-Peinado, N., Cortes-Serra, N., Torras-Claveria, L., Pinazo, M.J., Gascón, J., Bastida, J., and Alonso-Padilla, J. (2020). Amaryllidaceae alkaloids with anti-*Trypanosoma cruzi* activity. Parasit. Vectors. 13, 1–10. DOI: 10.1186/s13071-020-04171-6.

Martínez-Peinado, N., Cortes-Serra, N., Sherman, J., Rodríguez, A., Bustamante, J.M., Gascón, J., Pinazo, M.J., and Alonso-Padilla, J. (2021). Identification of *Trypanosoma cruzi* growth inhibitors with activity *in vivo* within a collection of licensed drugs. Microorganisms 9, 406. DOI: 10.3390/microorganisms9020406.

Menna-Barreto, R.F., Salomão, K., Dantas, A.P., Santa-Rita, R.M., Soares, M.J., Barbosa, H.S., and de Castro, S.L. (2009). Different cell death pathways induced by drugs in *Trypanosoma cruzi*: an ultrastructural study. Micron 40, 157–168.

DOI: 10.1016/j.micron.2008.08.003.

Morillo, C.A., Waskin, H., Sosa-Estani, S., Del Carmen Bangher, M., Cuneo, C., Milesi, R., Mallagray, M., Apt, W., Beloscar, J., Gascon, J., Molina, I., Echeverria, L.E., Colombo, H., Perez-Molina, J.A., Wyss, F., Meeks, B., Bonilla, L.R., Gao, P., Wei, B., and McCarthy, M. (2017). benznidazole and posaconazole in eliminating parasites in asymptomatic *T. cruzi* carriers: The STOP-CHAGAS trial. J. Am. Coll. Cardiol. 69, 939–947. DOI: 10.1016/j.jacc.2016.12.023.

Nair, J.J., and van Staden, J. (2023). Antiviral alkaloid principles of the plant family Amaryllidaceae. Phytomedicine 108, 154480. DOI:10.1016/j.phymed.2022.154480.

Ortiz, J.E., Pigni, N.B., Andujar, S.A., Roitman, G., Suvire, F.D., Enriz, R.D., Tapia, A., Bastida, J., and Feresin, G.E. (2016). Alkaloids from *Hippeastrum argentinum* and their cholinesterase-inhibitory activities: an in vitro and in silico study. J. Nat. Prod. 79, 1241–1248. DOI: 10.1021/acs.jnatprod.5b00785.

Soeiro, M.N., and de Castro, S.L. (2011). Screening of potential anti-*Trypanosoma cruzi* candidates: *in vitro* and *in vivo* studies. Open Med. Chem. J. 5, 21–30. DOI: 10.2174/1874104501105010021.

Souza, J.M., Vieira, T.M., Candido, A.C.B.B., Tezuka, D.Y., Rao, G.S., de Albuquerque, S., Crotti, A.E.M., Siqueira-Neto, J.L., and Magalhães, L.G. (2021). *In vitro* anti-*Trypanosoma cruzi* activity enhancement of curcumin by its monoketone tetramethoxy analog diveratralacetone. Curr. Res. Parasitol. Vector Borne Dis. 1, 100031. DOI: 10.1016/j.crpvbd.2021.100031.

Slanis, A.C., Huaylla, H., Ortiz, J.E., Luna, L.C., and Feresin, G.E. (2022). *Hippeastrum escoipense* (Amaryllidaceae, Amaryllidoideae): una nueva especie críptica del noroeste de Argentina. Darwiniana, Nueva Serie 10, 486–493. DOI: 10.14522/darwiniana.2022.102.1066.

Spina, R.M., Lozano, E., Barrera, P.A., Agüero, M.B., Tapia, A., Feresin, G.E., and Sosa, M.Á. (2018). Antiproliferative effect and ultrastructural alterations induced by 5-*O*-methylembelin on *Trypanosoma cruzi*. Phytomedicine 46, 111–118. DOI: 10.1016/j.phymed.2018.04.032.

Tallini, L.R., Giordani, R.B., de Andrade, J.P., Bastida, J., and Zuanazzi, J.A.S. (2021). Structural diversity and biological potential of alkaloids from the genus *Hippeastrum*, Amaryllidaceae: an update. Rev. Bras. Farmacogn. 31, 648–657. DOI: 10.1007/s43450-021-00211-z.

Tallini, L.R., Osorio, E.H., Santos, V.D.D., Borges, W.S., Kaiser, M., Viladomat, F., Zuanazzi, J.A.S., and Bastida, J. (2017). *Hippeastrum reticulatum* (Amaryllidaceae): Alkaloid profiling, biological activities and molecular docking. Molecules 22, 2191. DOI: 10.3390/molecules22122191.

Torrico, F., Gascón, J., Barreira, F., Blum, B., Almeida, I.C., Alonso-Vega, C., Barboza, T., Bilbe, G., Correia, E., Garcia, W., Ortiz, L., Parrado, R., Ramirez, J. C., Ribeiro, I., Strub-Wourgaft, N., Vaillant, M., and Sosa-Estani, S. (2021). New regimens of benznidazole monotherapy and in combination with fosravuconazole for treatment of Chagas disease (BENDITA): a phase 2, double-blind, randomised trial. Lancet Infect. Dis. 21, 1129–1140. DOI: 10.1016/S1473-3099(20)30844-6.

Torrico, F., Gascon, J., Ortiz, L., Alonso-Vega, C., Pinazo, M.J., Schijman, A., Almeida, I.C., Alves, F., Strub-Wourgaft, N., and Ribeiro, I. (2018). Treatment of adult chronic indeterminate Chagas disease with benznidazole and three E1224 dosing regimens: a proof-of-concept, randomised, placebo-controlled trial. Lancet Infect. Dis. 18, 419–430. DOI: 10.1016/S1473-3099(17)30538-8.

Villalta, F., and Rachakonda, G. (2019). Advances in preclinical approaches to Chagas disease drug discovery. Expert Opin. Drug Discov. 14, 1161–1174. DOI: 10.1080/17460441.2019.1652593.

Wilkinson, S.R., Temperton, N.J., Mondragon, A., and Kelly, J.M. (2000). Distinct mitochondrial and cytosolic enzymes mediate trypanothione-dependent peroxide metabolism in *Trypanosoma cruzi*. J. Biol. Chem. 275, 8220–8225. DOI: 10.1074/jbc.275.11.8220.

World Health Organization Neglected Tropical Diseases. Available online: https://www.who.int/news-room/fact-sheets/detail/chagas-disease-(american-trypanosomiasis)(accessed on march 2023)

.

Table legends

Extract/ compound	*T. cruzi*									Toxicity	
	Epimastigotes			Trypo + Amastigotes			Amastigotes			Vero	HepG2
	IC_{50}[a]	IC_{90}[b]	SI[c]	IC_{50}[a]	IC_{90}[b]	SI[c]	IC_{50}[a]	IC_{90}[b]	SI[c]	TC_{50}[d]	TC_{50}[d]
Bzn[e] (µM)	8.21± 1.4	21.22 ± 2.36	26.42	2.13 ± 0.12	7.84 ± 1.16	101.83	1.47 ± 0.08	6.27 ± 1.15	147.55	216.9 ± 71.69	203.5 ± 25.99
Bzn[e] (µg/ml)	2.14 ± 0.05	5.53 ± 0.41	26.66	0.56 ± 0.03	1.32 ± 1.07	101	0.33 ± 0.02	1.23 ± 1.21	146.18	57.06 ± 3.11	53.12 ± 6.39
AE-*H. escoipense* (µg/ml)	2.63 ± 0.87	5.91 ± 0.34	11.51	1.62 ± 0.09	3.39 ± 1.31	18.72	1.53 ± 0.09	2.49 ± 1.09	21.32	30.28 ± 3.28	10.34 ± 1.20
Cnd (µM)	4.28 ± 0.47	10.31 ± 0.73	59.67	2.49 ± 0.16	6.12 ± 1.15	102.57	1.60 ± 0.15	6.59 ± 1.17	159.63	255.4 ± 74.93	85.17 ± 15.49
Cnd (µg/ml)	1.48 ± 0.18	3.56 ± 0.23	59.59	0.86 ± 0.06	2.11 ± 0.12	102.54	0.55 ± 0.04	2.28 ± 0.17	160.34	88.19 ± 21.32	29.41 ± 4.47

Table 1. Antiparasitic and cytotoxic activities of the AE-*H. escoipense*, Cnd, and Bzn.

[a], half-maximal inhibitory concentration. [b], 90 % inhibitory concentration. [c], selectivity index over Vero cells (TC_{50}/IC_{50}). [d], half-maximal toxic concentration. [e], positive control.

Table 2. CI values and respective Fa and DRI of various combinations of Cnd (C) and Bzn (B). CI in green indicates synergetic interaction.

Cell type	Concentration (µM C + µM B)	CI	Fa	DRI	
Epimastigotes	1.07 + 2.05	0.841	0.407	C = 3.19	B = 1.89
	2.14 + 4.10	1.104	0.555	C = 2.07	B = 1.61
	4.28 + 8.21	1.812	0.625	C = 1.17	B = 1.05
	8.56 + 16.42	1.605	0.856	C = 1.01	B = 1.63
	17.12 + 32.84	1.751	0.944	C = 0.79	B = 2.07
Trypomastigotes + Amastigotes	0.60 + 0.47	1.056	0.258	C = 2.41	B = 1.56
	1.21 + 0.94	1.030	0.456	C = 2.32	B = 1.67
	2.41 + 1.87	0.999	0.670	C = 2.26	B = 1.79
	4.82 + 3.74	0.867	0.850	C = 2.45	B = 2.18
	9.64 + 7.48	0.979	0.920	C = 2.08	B = 2.01
Amastigotes	0.40 + 0.37	0.859	0.232	C = 3.18	B = 1.84
	0.80 + 0.74	1.272	0.326	C = 2.17	B = 1.23
	1.60 + 1.47	1.190	0.616	C = 2.39	B = 1.29
	3.20 + 2.94	0.731	0.912	C = 4.08	B = 2.06
	6.40 + 5.88	0.080	0.999	C = 41.52	B = 17.57
Vero	0.60 + 0.47	> 3	0.245	C = 1.03	B = 5.21E-4
	1.21 + 0.94	> 3	0.232	C = 1.28	B = 0.002
	2.41 + 1.87	> 3	0.217	C = 1.87	B = 0.01
	4.82 + 3.74	> 3	0.204	C = 2.38	B = 0.04
	9.64 + 7.48	> 3	0.217	C = 0.46	B = 0.003
HepG2	0.60 + 0.47	> 3	0.065	C = 2.1E-13	B = 0.008

1.21 + 0.94	> 3	0.137	C = 0.59	B = 0.71
2.41 + 1.87	1.255	0.153	C = 33.10	B = 0.82
4.82 + 3.74	> 3	0.114	C = 8.31E-5	B = 0.048
9.64 + 7.48	2.466	0.168	C = 414.33	B = 0.41

CI, combination index. Fa, fraction affected. DRI, doses reduction index.(Chou, 2010, Chen *et al*., 2023)

Figure legends

Figure 1. Effect of AE-*H. escoipense* in the proliferation of epimastigotes (Dm28c strain) of *T. cruzi*. Values are expressed as means ± SD after 24, 48 or 72 h of incubation. *, **, ***, respectively indicate the differences observed were statistically significant from the negative control at $p < 0.05$, $p < 0.01$, and $p < 0.001$.

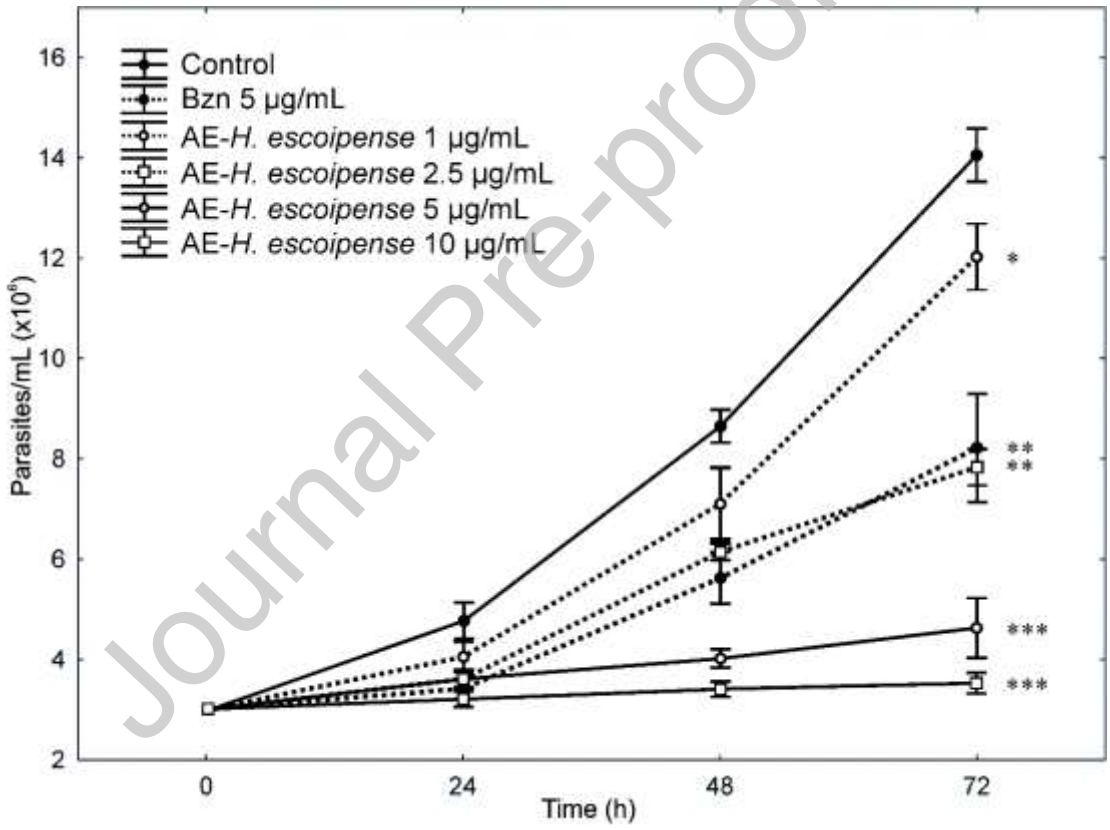

Figure 2. Concentration-response curves of AE-*H. escoipense* (red triangles) and Bzn (black circles). (A) Anti-trypomastigotes+amastigotes assay. (B) Vero cells toxicity assay. (C) HepG2 cells toxicity assay. (D) Anti-amastigote assay.

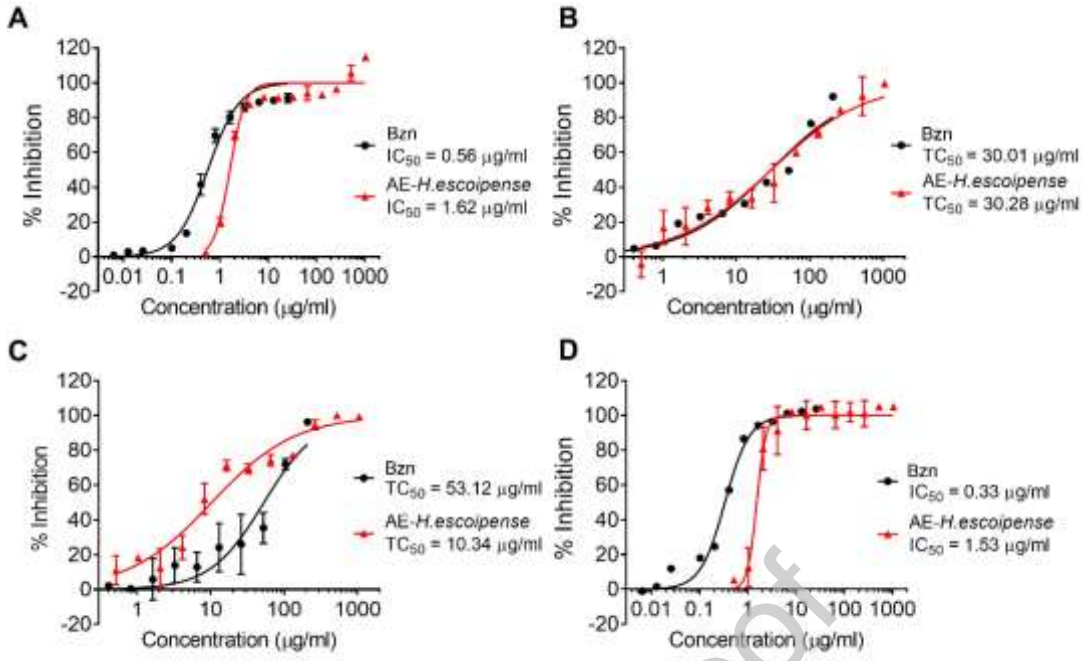

Figure 3. Candimine

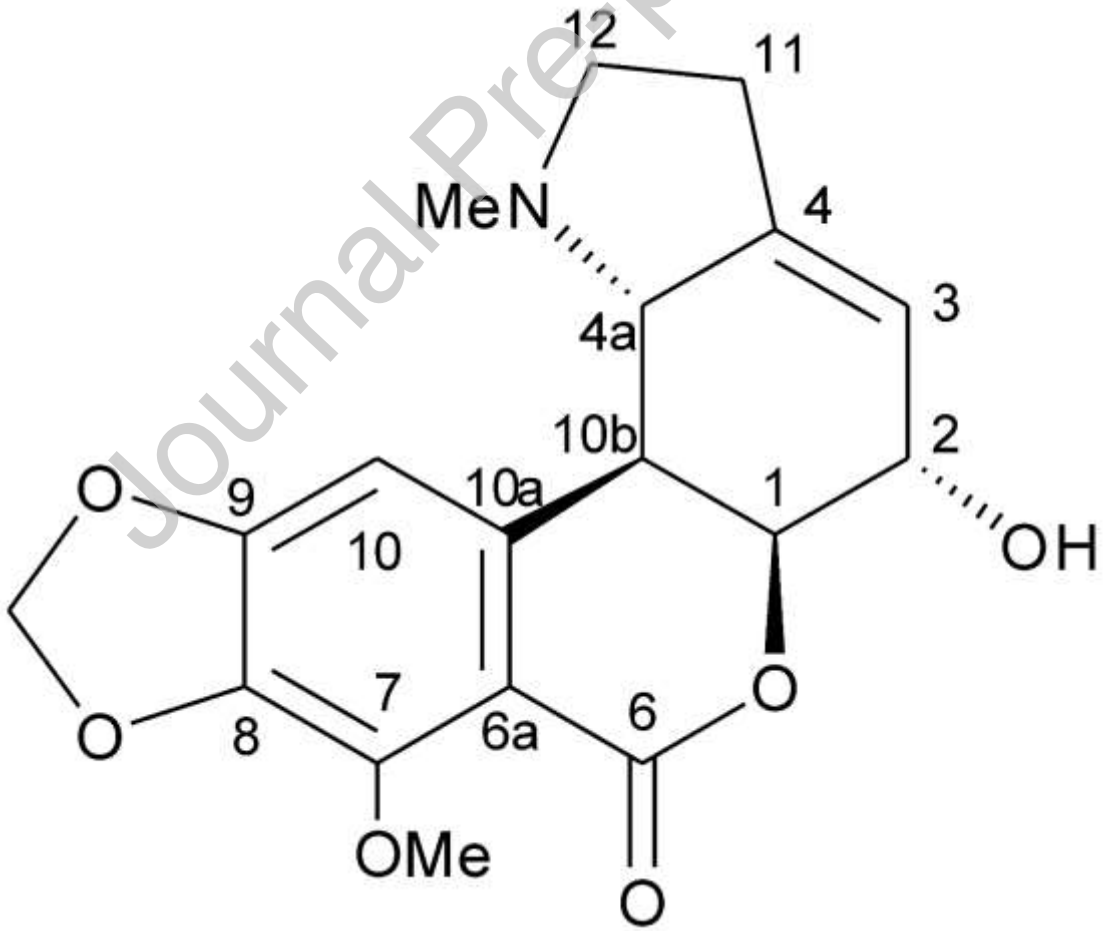

Figure 4. Effect of Cnd in the proliferation of epimastigotes (Dm28c strain) of *T. cruzi*. Values are expressed as means ± SD after 24, 48 or 72 h of incubation. *;**;*** = significantly different from the negative control ($p < 0.05$, $p < 0.01$, $p < 0.001$, respectively).

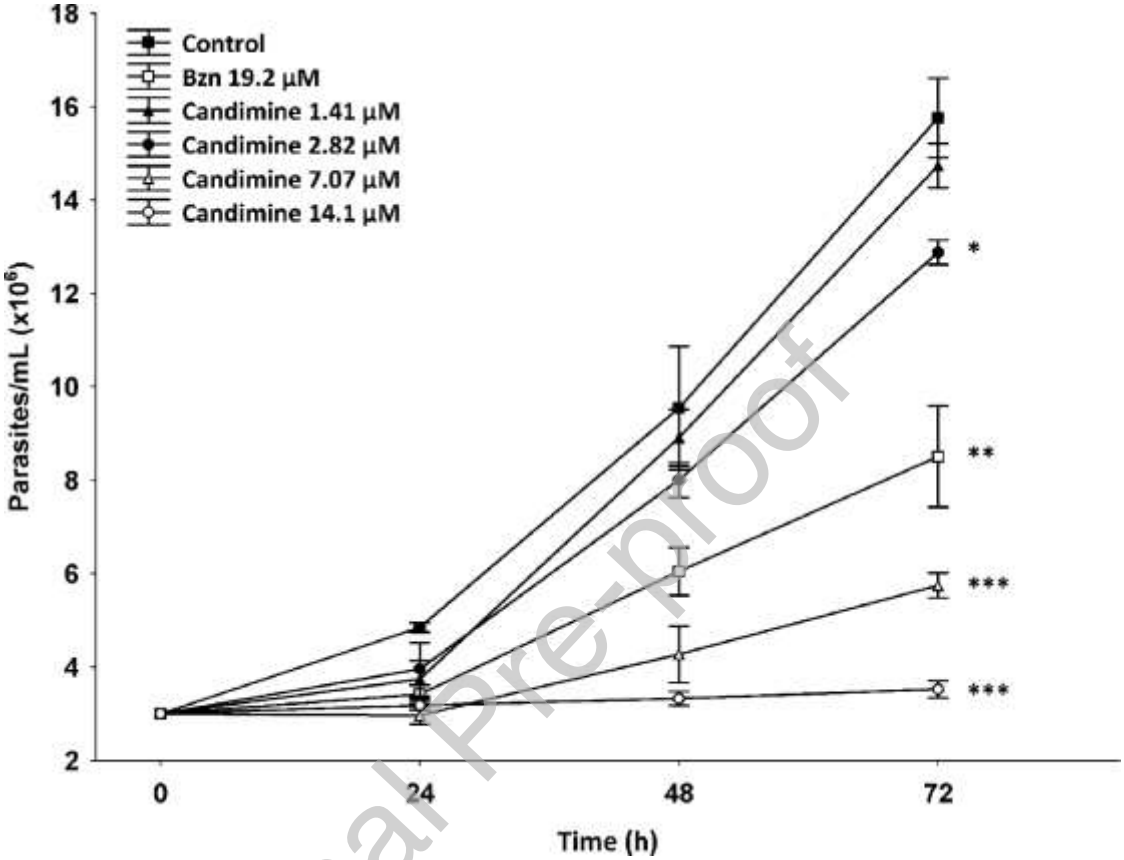

Figure 5. Concentration-response curves of Cnd (red triangles) and Bzn (black circles). (A) Anti-trypomastigotes+amastigotes assay. (B) Vero cells toxicity assay. (C) HepG2 cells toxicity assay. (D) Anti-amastigote assay.

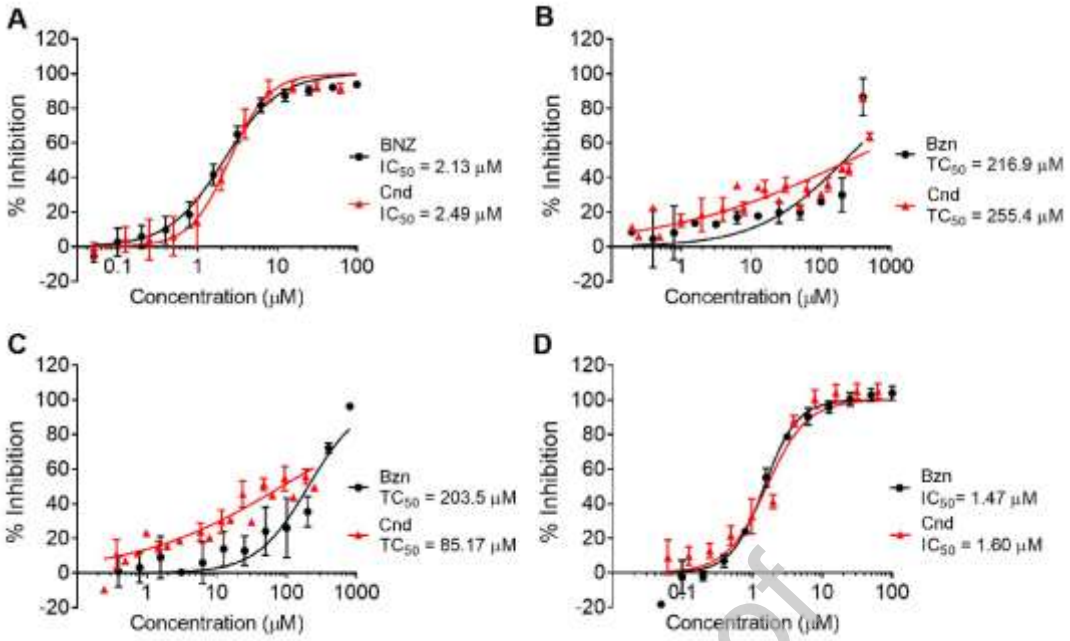

Figure 6. Transmission electron micrograph of *T. cruzi* epimastigotes untreated (A) and treated with 7.07 µM (B) and 14.1 µM (C) of Cnd. N: nucleus; K: kinetoplast; M: mitochondria; R: reservosomes-like structures; Ac: acidocalcisosome *: vacuoles; black arrows: membrane blebs.

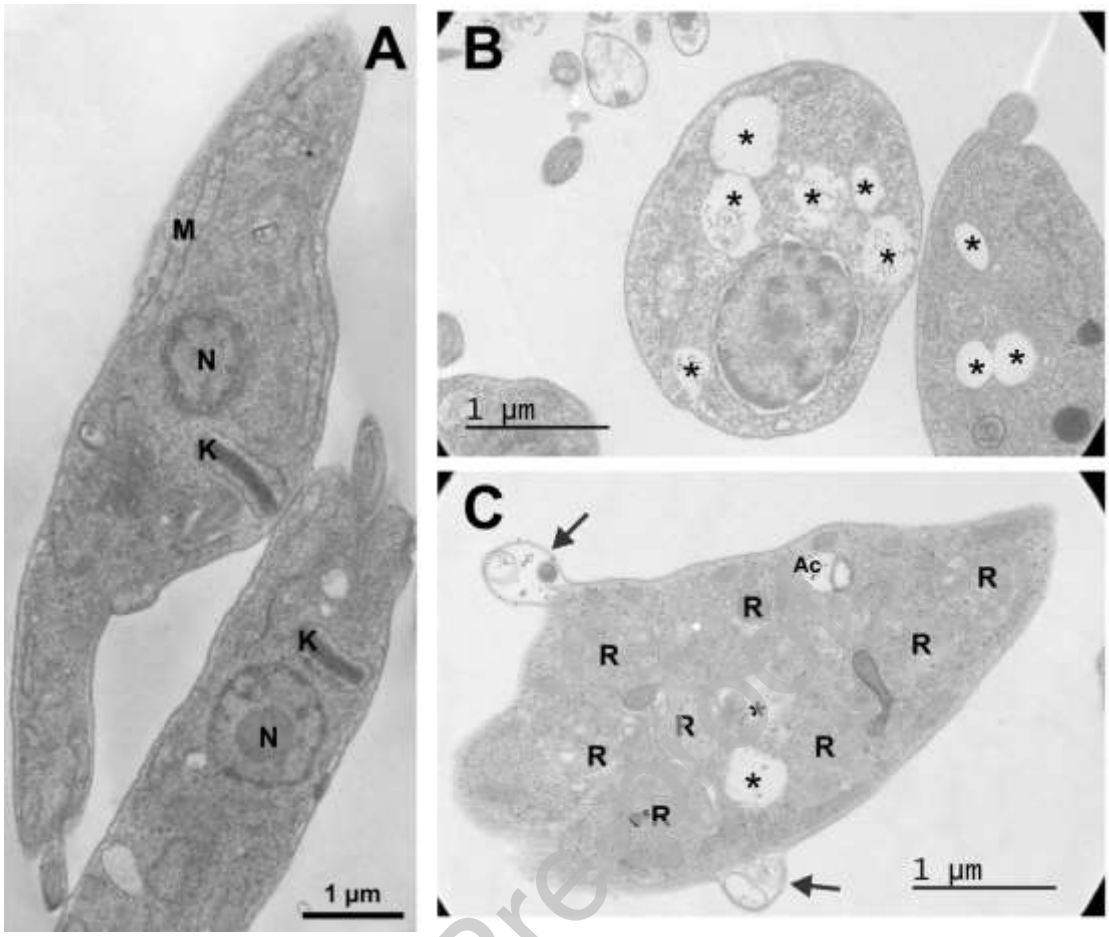

Figure 7. Effect of Cnd (28.3 µM) on the mitochondrial activity of *T. cruzi* epimastigotes at 48 h. *: significantly different from the control ($p < 0.05$).

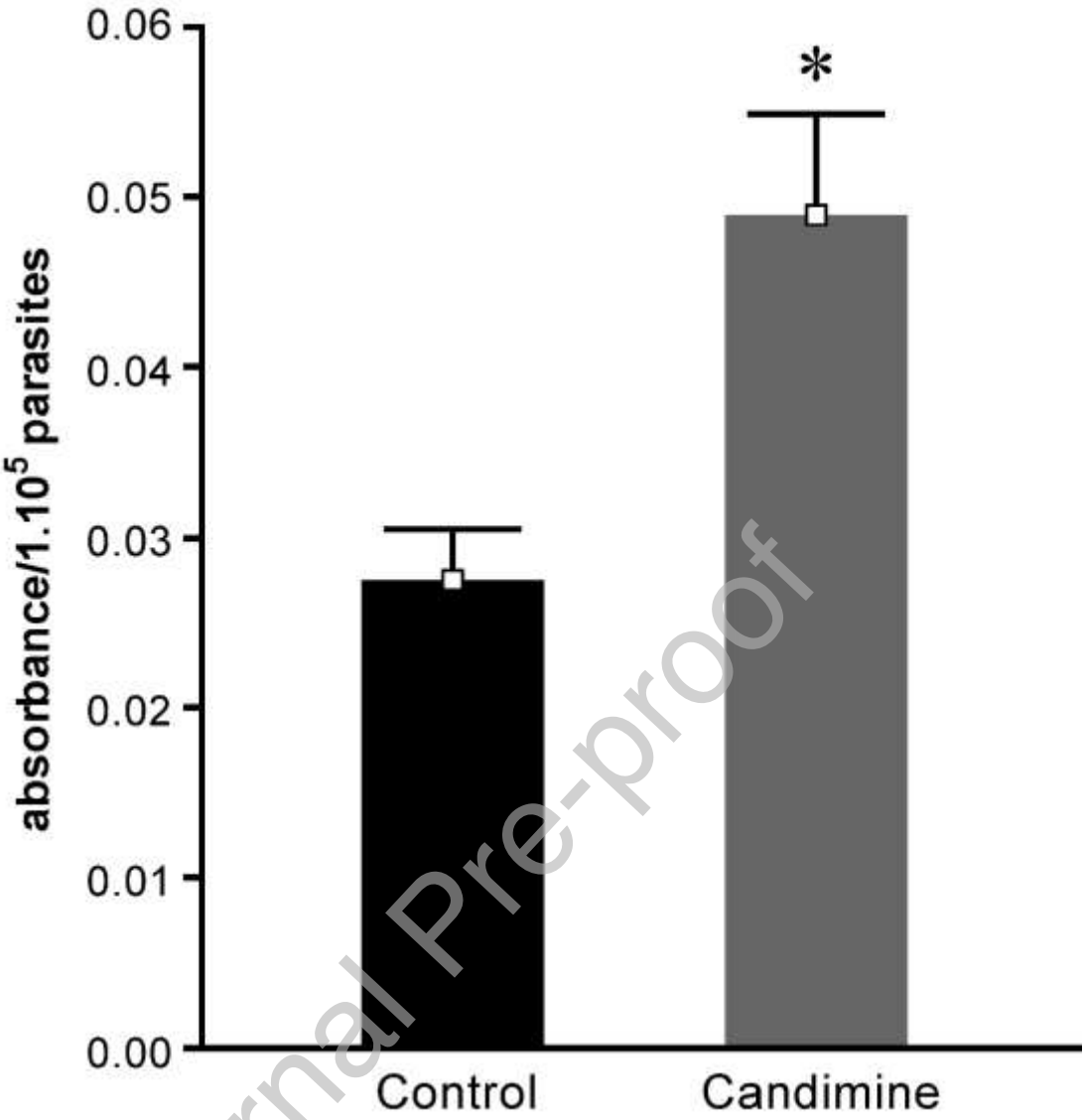

Figure 8. Graphic representations obtained from the CompuSyn report for Cnd and Bzn and their combinations in epimastigotes, trypomastigotes+amastigotes, and amastigotes (left, middle and right, respectively). (A, B, C) Concentration-effect curve demonstrates the relationship between Fa and Concentration. (D, E, F) The Fa-CI plot represents synergistic, additive, or antagonistic interactions (CI < 1, CI = 1, CI > 1, respectively) based on their inhibitory effect (Fa). (G, H, I) In the Fa-DRI plot, data points appearing below the line of no concentration reduction (DRI = 1) indicate an unfavourable concentration reduction, while those above the line indicate a favourable concentration reduction.

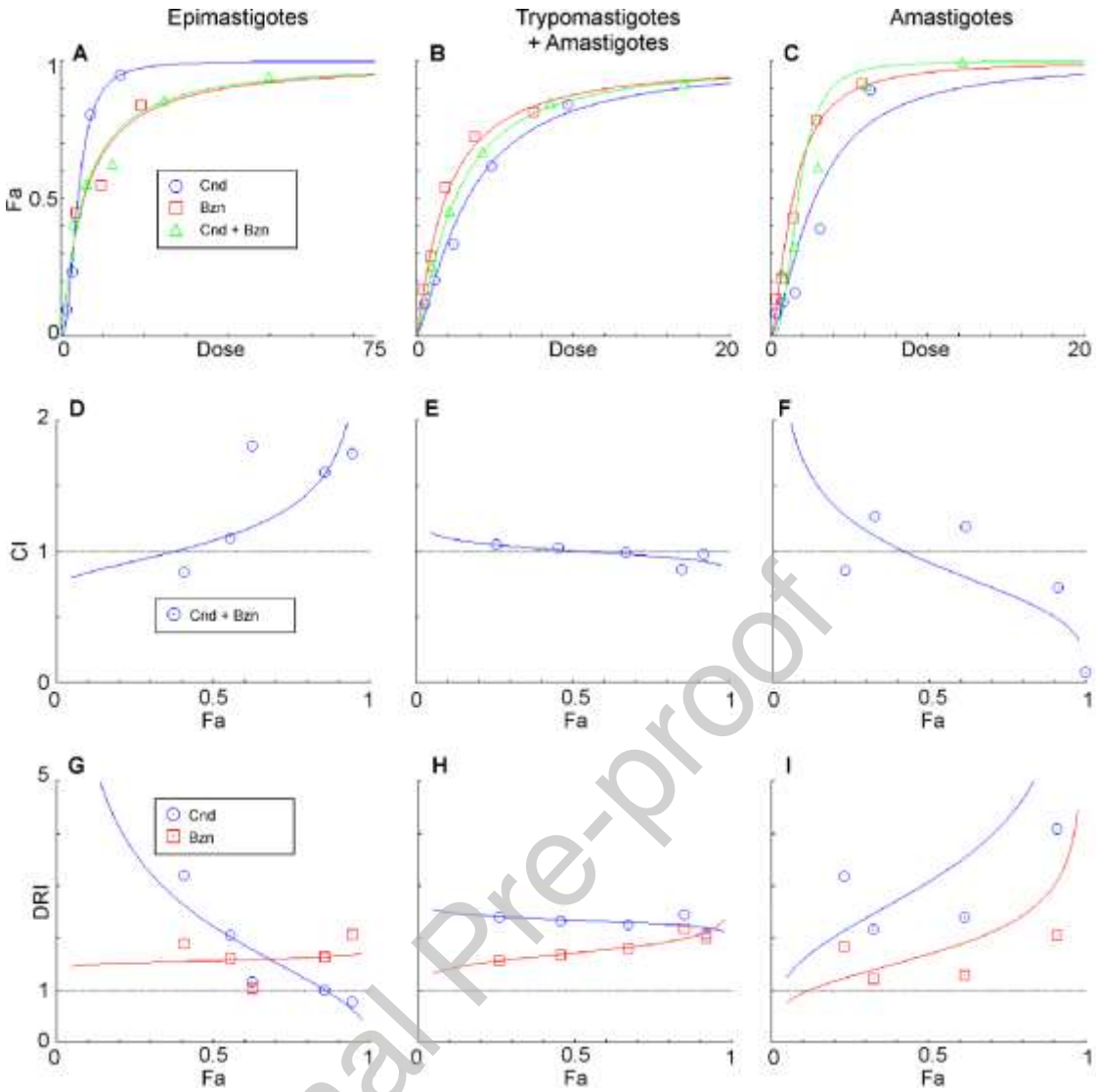

Figure 9. Heat map from CI values. The squares indicate synergism (CI < 1, green), additivism (1 = CI, yellow), or antagonism (CI > 1, orange-red) between Cnd and Bzn against *T. cruzi* (epimastigotes, trypomastigotes+amastigotes, and amastigotes) and mammalian cells (Vero and HepG2) at combination setting described in Fig. S1.

Credit authorship contribution statement

JEO, MP, MAS, JAP and GEF conceptualized the study. MP, NMP and PAB performed biological assays. JEO, JB and GEF performed chemical studies and provided the extract and purified alkaloids. JEO, MP, JAP, GEF and JB wrote the article. All authors agree to be accountable for all aspects of work ensuring integrity and accuracy.

Declaration of Competing Interest

The authors declare no conflict of interest. The funders had no role in the design of the study; in the collection, analyses, or interpretation of data; in the writing of the manuscript, or in the decision to publish the results.

Funding

We thank the support of the Generalitat of Catalonia Universities and Research Department, Spain (AGAUR; 2017SGR00924). This work was partially supported by ANPCyT (PICT-2020-SERIEA-03883), CONICET-PIP 11220210100902CO, and CICITCA-UNSJ (Argentina), BIFRENES RED 416RT0511 and RENATEC RED P22RT0127 (CYTED Spain). This work also received funding from the Carlos III Health Institute (ISCIII), RICET Network for Cooperative Research in Tropical Diseases (ISCIII; RD16/0027/0004), and FEDER. We also acknowledge support from the Spanish Ministry of Science, Innovation, and Universities through the "Centro de Excelencia Severo Ochoa 2019–2023″ Program (CEX2018–000,806-S), and from the Generalitat of Catalonia through the "CERCA Program".

Data availability statement

All data generated or analysed during this study are included in this published article (and its Supplementary Information files).